Preparation and Characterization of Organoclay-Rubber Nanocomposites via a New Route with Skim Natural Rubber Latex

Rosamma Alex,* Changwoon Nah

Department of Polymer Science and Technology, Chonbuk National University, Jeonju 561-756, South Korea

Received 27 October 2005; accepted 31 March 2006
DOI 10.1002/app.24738
Published online in Wiley InterScience (www.interscience.wiley.com).

ABSTRACT: Skim natural rubber latex (SNRL) is a protein rich by-product obtained during the centrifugal concentration of natural rubber (NR) latex. A new method to recover rubber hydrocarbon and to obtain nanocomposites with organoclay (OC) was investigated. The approach involved treatment of SNRL with alkali and surfactant, leading to creaming of skim latex and removal of clear aqueous phase before addition of OC dispersion. Clay mixed latex was then coagulated to a consolidated mass by formic acid, followed by drying and vulcanization like a conventional rubber vulcanizate. X-ray diffraction (XRD) studies revealed that NR nanocomposites exhibited a highly intercalated structure up to a loading of 15 phr (parts per hundred rubber) of OC. Transmission electron microscopy studies showed a highly exfoliated and intercalated structure for the NR nanocomposites at loadings of 3–5 phr organically modified montmorillonite (OMMT). The presence of clay resulted in a faster onset of cure and higher rheometric torque. The rubber recovered from skim latex had a high gum strength, and a low amount of OC (5 phr) improved the modulus and tensile strength of NR. The high tensile strength was supported by the tensile fractography from scanning electron microscopy. Thermal ageing at 70°C for 6 days resulted in an improvement in the modulus of the samples; the effect was greater for unfilled NR vulcanizate. The maximum degradation temperature was found to be independent of the presence and concentration of OC. The increased restriction to swelling with the loading of OC suggested a higher level of crosslinking and reinforcement in its presence. J Appl Polym Sci 102: 3277–3285, 2006

Key words: rubber; organoclay; nanocomposites; particle size distribution; TEM

INTRODUCTION

Natural rubber (NR) obtained from the latex of *Hevea Braziliensis* tree has been the most widely accepted rubbery material because of its excellent gum strength, elasticity, and low temperature performance. Rubber is present in latex as a colloidal dispersion of spherical or pear shaped rubber particles with size in the range of 50 Å to 3 μm in an aqueous serum.[1–2] The rubber particle contains hundreds of molecules of rubber hydrocarbon and is surrounded by a surface film of various kinds of lipids and proteins that provide colloidal stability to the aqueous dispersion.[3–5]

The rubber content of latex, which is around 30–40% by weight, is generally increased to about 60% in commercial concentrated latex by centrifugation. During this process, large quantities of a protein-rich serum called skim latex containing 4–8% rubber are released as a by-product. The low particle size and presence of higher quantity of nonrubber ingredients cause problems in recovering rubber hydrocarbon from skim latex.[6] The dirt content of skim latex is low and should no doubt be a source of high quality rubber if the protein content is reduced and problems arising from coagulation are solved. Normally, rubber is recovered either by spontaneous coagulation or coagulation using chemicals such as dilute sulfuric acid[7] or quaternary ammonium salts.[8] Use of ammonium stearate is reported to be beneficial in enhancing the formation of a firmer coagulum. The protein content of skim is generally reduced by enzymatic protein hydrolysis.[9] A creaming process using inorganic salts in the presence of enzymes has been reported for production of good quality skim rubber.[10]

Rubber-based materials require reinforcement from the fillers added during their processing, and the recent approach has been to use nanosize fillers at reduced quantities for enhancement of properties.[11–13] For several decades carbon black and silica with particle size 10–30 nm had been used successfully for reinforcement of NR. Much effort is being carried out to replace carbon black or silica by a new class of ex-

Correspondence to: R. Alex (rosammaalex2000@yahoo.com)
**Present address*: Rubber Research Institute of India, Kerala, India.

Contract grant sponsor: KOFST and KOSEF under Brain Pool programme 2004 (042-4-11).

tensively studied filler called montmorollinite (MMT) clay[13–15] which can be modified with quaternary ammonium salts to give organically modified montmorillonite (OMMT) or organoclay (OC). Treatment of MMT for ion exchange reactions using cationic surfactants make them more hydrophilic with increased inter layer distance. Such modified clay shows unique reinforcement characteristics as polymer molecules can travel into the interlayer spacing of clays.[16–20] Organoclay is incorporated into rubber either by dry mixing[21,22] or by addition to rubber in solution, at molten or latex stage.[23–26] Mixing nanochemicals in the latex stage and co-coagulating has been shown recently as more environmental friendly and a simple process to obtain reinforcement characteristics.[27] Addition of chemicals in the latex stage, followed by further processing, definitely has the unique advantage of excellent dispersion and less molecular weight reduction.[28]

The important source of NR in the past had always been mostly block rubber, sheet rubber, and concentrated latex. Even though skim latex is produced in large quantities and is environmentally desirable to process it, the potential of it as an excellent source of NR is yet to receive appropriate attention.

In this article a new route for producing NR nanocomposites from a comparatively cheap source of NR by an environmentally friendly process is presented.

MATERIALS AND METHODS

The skim latex was obtained from Southland Latex Company, Thailand. The specifications of skim latex used are shown in Table I. Natural montmorillonite (MMT) modified with a quaternary ammonium salt (organoclay (OC)) [Cloisite-15A] was supplied by Southern Clay products, Texas, USA. The other chemicals used were commercial rubber grade chemicals.

Preparation of rubber–clay nanocomposite

The skim latex (as per quality parameters in Table I) was mixed with surfactant and alkali at definite concentrations for a definite period of time as reported earlier.[29] During this time, the proteins underwent hydrolysis to produce polypeptides and amino acids. Simultaneously, the adsorption of surfactant on the rubber particles also took place, which led to a creaming process. DRC increased to about 9.6%, with the separation of an aqueous serum layer that could be easily removed (Fig. 1). An aqueous (30%) dispersion of OC (Cloisite 15A), prepared by the addition of a small amount of surfactant (1% w/w of solid clay), was added to the creamed skim latex after removal of the serum and mixed for 15 min using a laboratory type mechanical stirrer while maintaining the temperature at 35°C. The clay dispersion was added so as to have concentrations of 1, 3, 5, 10, and 15 phr OC in the dried rubber. The creamed skim latex mixed with OC at the required concentration was coagulated by the addition of formic acid. The coagulated mass (coagulum, Fig. 2) was washed with distilled water until free of acid and then dried in an air oven at 70°C for 24 h. On addition of acid, the latex coagulated as a consolidated mass (Fig. 2), and the dried rubber had a pale yellow color (Fig. 3). The dried coagulum was mixed with all the required compounding ingredients as shown in Table II. The amount of NR shown excluded the amount of clay added in various formulations.

The rubber compounds, after mixing, were vulcanized at 150°C to their optimum cure time (t_{90}) determined using an oscillating-die rheometer (ODR; Alpha technologies, USA). The vulcanization was carried

TABLE I
Test Report of Skim Latex

Parameter	Test value
Dry rubber content	4.81
Ammonia content	0.49
pH	10.58

Figure 1 Photograph showing creaming process of skim natural rubber latex. [Color figure can be viewed in the online issue, which is available at www.interscience.wiley.com.]

Figure 2 Photograph of the organoclay filled wet coagulum. [Color figure can be viewed in the online issue, which is available at www.interscience.wiley.com.]

out at 150°C using a hydraulically operated press with electrically heated platens.

Characterization methods

Particle size of rubber latex was determined using a particle size analyzer model Microtrac, UPA 150, USA, using light scattering technique, which measures the quantity of light at predetermined angles scattered by the particles. X-ray diffraction (XRD) evaluation of the *d*-spacing (i.e., interlamellar or basal or *d*-spacing) between the silicate layers was by using Bragg's law[30] given below.

$$n\lambda = 2d \sin\theta \tag{1}$$

XRD data between 2 and 10° were obtained at 4° min^{-1} on a diffractometer (Rigaku 2500 PC, Japan) with Cu Kα radiation (wave length, 1.54 Å) at a generator voltage of 40 kV and a generator current of 40 mA. Transmission electron microscopy (TEM) images were taken from cryogenically microtomed ultrathin sections using a ZEISS EFTEM (model: EM 912 OMEGA H-800) operating at 120 kV.

Figure 3 Photograph of the organoclay filled dry coagulum. [Color figure can be viewed in the online issue, which is available at www.interscience.wiley.com.]

TABLE II
Formulation of the Mixes

Ingredient	phr
NR (dry)	100
Zinc oxide	5
Stearic acid	1
Antioxidant (NS)*	1
CBS**	0.9
Sulfur	2.5

*NS-(TDQ) (polymerized 2,2,4-trimethyl-1,2-dihydroquinoline).
**CBS, *N*-cyclohexy2 benzothiazolesulfenamide.

The cure characteristics of the rubber compounds were determined using an ODR at different temperatures such as 150, 160, and 170°C. The energy of activation E_{act} of curing was determined using the Arrhenius equations given below.

$$k = A \exp(-E_{act}/RT) \tag{2}$$

$$\log k = \log A - E_{act}/2.303RT \tag{3}$$

where, A is the Arrhenius constant, E_{act} the activation energy, R the universal gas constant, T the absolute temperature, and k the cure reaction rate constant. The rate constant is determined from rheograph as given below.

$$\ln (M_h - M_t) = -kt + \ln (M_h - M_n) \tag{4}$$

where M_h is the maximum rheometric torque, M_n the minimum rheometric torque, M_t rheometric torque at time t, and k the cure reaction rate constant.

The slope of the plot of ln ($M_h - M_t$) versus time t from the rheograph directly gives the value of cure reaction rate constant k.

The tensile and tear strength of the samples were tested using a tensile tester (model LRX plus, Lloyd Instruments, UK), at 500 mm/min, as per ASTM D 412-80. Ageing characteristics were determined by measurement of tensile strength of dumb bell samples placed in a laboratory-size air oven maintained at 70°C for 6 days. Shore A hardness of the samples was determined using a Shore A hardness durometer ASKER, Japan, as per ASTM D 2240.

The thermal stability of the samples were determined using thermograms recorded on a thermogravimetric analyzer (model TGA-Q-50, TA Instruments) at a heating rate of 10°C/min under N_2 atmosphere.

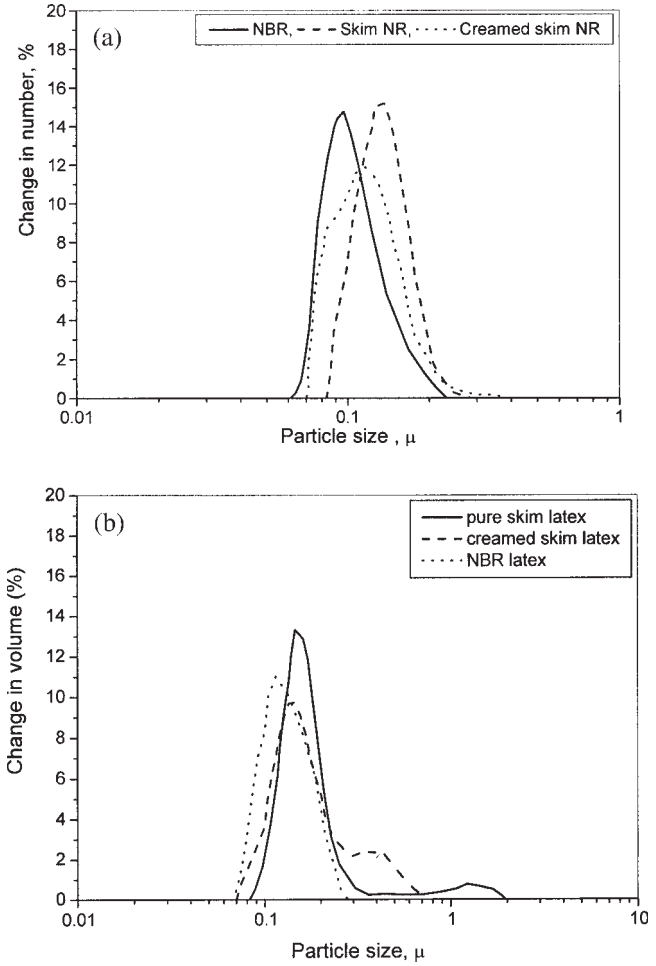

Figure 4 (a) Graph of incremental total number (%) versus size of particle. (b) Graph of incremental total volume (%) versus size of particle.

The SEM fractography of the samples was taken on a scanning electron microscope (SEM), model JEOL JSM-6400, Japan, at 20 kV using sputter-coated samples.

TABLE III
Particle Size Analysis Data

Percentage of the particles	Size range (μm) Before creaming	After creaming
15	≥0.1060	≥0.0865
20	≥0.1105	≥0.0907
35	≥0.1225	≥0.1029
40	≥0.1262	≥0.1069
50	≥0.1335	≥0.1150
60	≥0.1413	≥0.1237
70	≥0.1502	≥0.1337
80	≥0.1614	≥0.1464
90	≥0.1782	≥0.1674
95	≥0.1946	≥0.1895
Mean average size	*0.1689*	*0.1601*
Number average size	*0.1390*	*0.1233*

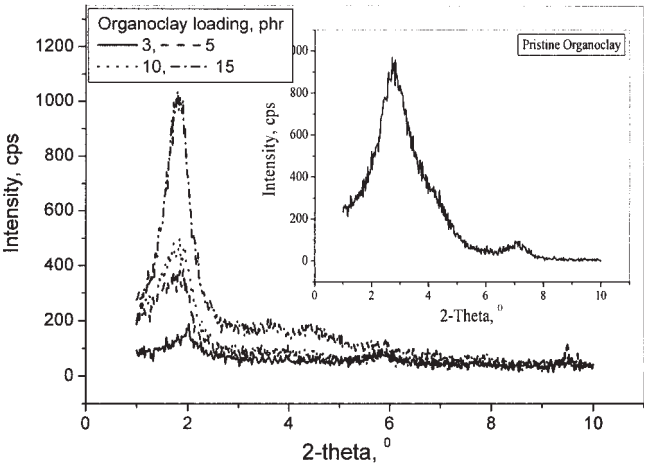

Figure 5 XRD spectra of pure MMT and NR nanocomposite containing 3, 5, 10, and 15 phr organoclay.

Swelling characteristics were measured by swelling circular samples in toluene at 20°C.

RESULTS AND DISCUSSION

Particle size distribution

The particle size distribution of neat skim latex and after subjecting it to creaming in comparison with a commercial synthetic latex (acrylonitrile butadiene rubber latex) is shown in Figures 4(a) and 4(b). The particle size varies from 0.0937 to 0.6304 μm for pure skim latex, and there is a noticeable overall reduction in particle size after creaming where the variation is from 0.0788 to 0.5781 μm based on number distribution (Table III). It is interesting to note that more than 14% of the particles after creaming recorded a size lower than the smallest detected particles of pure skim rubber latex. The size variation based on volume distribution of rubber particle varies from 0.0937 to 1.783 μm for skim natural rubber latex (SNRL) and 0.0788 to 0.6304 μm for creamed SNRL. Particle size obtained here is in close agreement with the earlier reported values on particle size of skim latex, which is shown to be about 0.1 μm[10] or in the range of 0.072–0.995 μm.[31] As expected, this is below the average particle size of fresh latex, since larger particles are known to readily

TABLE IV
XRD Data of NR Nanocomposites

Sample	2θ°	*d* (Å)
Organoclay	2.76	31.96
Organoclay (phr) in NR		
3	2	44.11
5	1.84	47.95
10	1.84	47.95
15	1.80	49.02

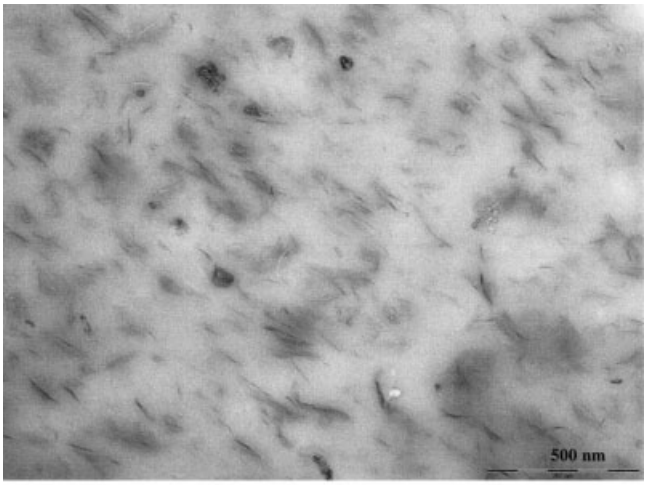

Figure 6 TEM image of NR mixed with 3 phr OMMT at two different magnifications: (a) low magnification, (b) high magnification.

separate into concentrated fraction. The particle size of fresh *Hevea* latex was shown to have a bimodal distribution with a mean diameter of 1.07 μm[32] and in some cases a lower size range of 0.08–0.75 μm.[32–34] During the creaming process, it is expected that the proteins adsorbed on rubber particles undergo hydrolysis. The reduction in size of the particles could be attributed to this process because the protein envelope that surrounds the rubber particle and that confers colloidal stability has been reported to be ~100 Å thick.[35] Thus during the process of creaming the size distribution of NR particles is reduced to the range of synthetic rubber latex.

X-ray diffraction studies

Figure 5 represents XRD spectra for NR nanocomposites obtained from skim NR latex. The basal spacing of 001 plane for Cloisite 15A is 3.15 nm, corresponding to a 2θ value of 2.86.[36] The change in the basal spacing for NR nanocomposites as represented by a change in the position of the peak from that of pure OC is shown in Table IV. The basal spacing of organically modified MMT increases in the NR clay nanocomposite, showing that there is pronounced insertion of NR molecules in the clay galleries, leading to the formation of a highly intercalated matrix. This distance increases to 47.95 Å at a loading of 5 phr clay and to 49.02 A units at a loading of 15 phr. The extent of intercalation is found to vary with different batches of skim latex. It was observed that for nanocomposites prepared from a batch of skim latex (of DRC%, 5.8) the intergallery spacing increased to 47.4 nm by addition of 1 or 2 phr of OMMT. Although the extent of intercalation is affected by factors such as diffusion of elastomer chains within silicate galleries, nature of elastomer, etc.,[37] it is thought to be independent of filler concentration.

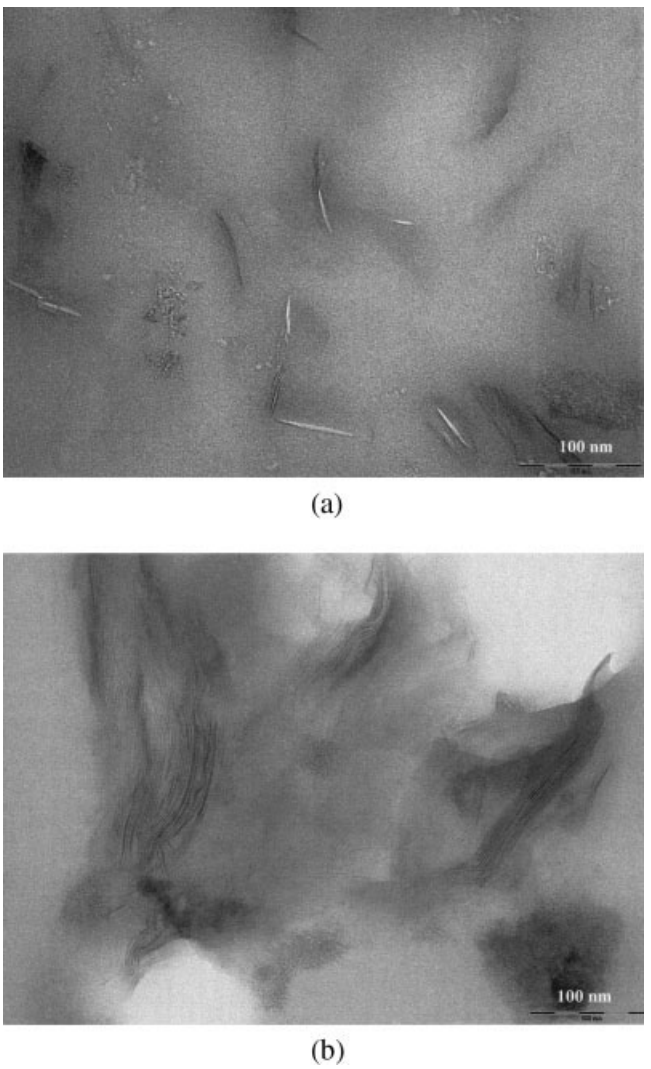

Figure 7 TEM images of NR nanocomposites (a) with 3 phr OMMT, (b) with 5 phr OMMT.

TABLE V
Characteristics of Skim NR Nanocomposites (from Rheographs at 150°C)

Cure property	Loading of clay (phr)				
	0	3	5	10	15
Minimum torque (dN m)	0.70	0.94	1.25	1.27	1.68
Maximum torque (dN m)	17.71	18.32	18.99	20.34	21.70
Optimum cure time (min)	11.73	11.59	11.17	10.48	9.88
Induction time, t_{s1} (min)	4.02	2.53	1.93	1.71	1.28
Scorch time, t_{s2} (min)	4.40	3.0	2.52	2.18	1.63

However, there are reports stating that this intergallery distance is reduced at higher loading of clay[10,38] attributed mainly to squeezing of silicate layers by polymer molecules during crosslinking process.[39]

Transmission electron microscopy

Direct evidence for homogeneous dispersion of clay in NR matrix is derived from TEM micrographs shown in Figures 6and 7. The low magnification TEM images of NR nanocomposites with 3 phr OMMT [Fig. 6(a)], in which silicate layers are shown as dark lines, display that even though in some areas the silicate layers are staked up, they are highly exfoliated in some other areas. This is more obvious in the higher magnification TEM image [Fig. 6(b)]. A higher loading of OMMT (in addition to a loading of 3 phr) also displays well-dispersed structure showing mostly intercalated along with exfoliated matrices, as observed from Figures 7(a) and 7(b). The peeling apart of platelet stacks observed for high molecular mass polymer/layered silicate systems are clearly seen at a higher loading of 5 phr. Thus NR chains, because of their very high segmental mobility, are able to intercalate into the gap very easily and cause exfoliation.

Cure characteristics

The processing characteristics are shown in Table V. A high level of rheometric torque, that is a measure of crosslinking, is observed for pure NR. The optimum cure time, scorch time, and induction time show a progressive drop with addition of OMMT, showing that the onset of cure is faster in its presence. This is obviously related to the transition complex formation with amines and sulfur, which accelerate curing process, in the first step of curing reaction. Comparatively high acceleration of cure for rubber vulcanizates in the presence of clay has been reported for NR[17,21] and epoxidized NR.[40] Both the maximum and minimum torque also record a marginal increase with filler loading, suggesting a higher level of crosslinking in the presence of clay. The temperature sensitivity of vulcanization is slightly less for clay-filled compounds than for pure NR as obtained from activation energy of vulcanization E_a calculated from the rate of vulcanization. The values of E_a were 93.54, 85.53, 90.36, 91.05, 91.54 kJ/mol, respectively, for 0, 1, 3, 5, 10, and 15 phr clay containing compounds.

Mechanical properties

The mechanical properties of NR nanocomposites are given in Table VI. The rubber hydrocarbon recovered from skim latex shows very high gum strength, suggesting that rubber obtained from skim latex has higher molecular weight. As observed from particle size distribution, skim latex has smaller particles when compared with centrifuged latex. It has been suggested in previous reports that higher molecular weights were associated with smaller rubber particles.[41,42] Among different rubber yielding plants also it was observed that latex with lower particle

TABLE VI
Mechanical Properties of Skim NR

Parameter	Loading of clay (phr)				
	0	3	5	10	15
Modulus, 100% (MPa)	1.62	1.98	2.11	2.79	2.98
Modulus, 200% (MPa)	2.24	2.59	2.73	3.63	3.67
Modulus, 300% (MPa)	2.78	3.23	3.30	4.5	4.63
Tensile strength (MPa)	22.54	24.57	25.79	24.8	24.18
Elongation at break (%)	770	730	780	710	700
Hardness (Shore A)	55	60	65	70	76

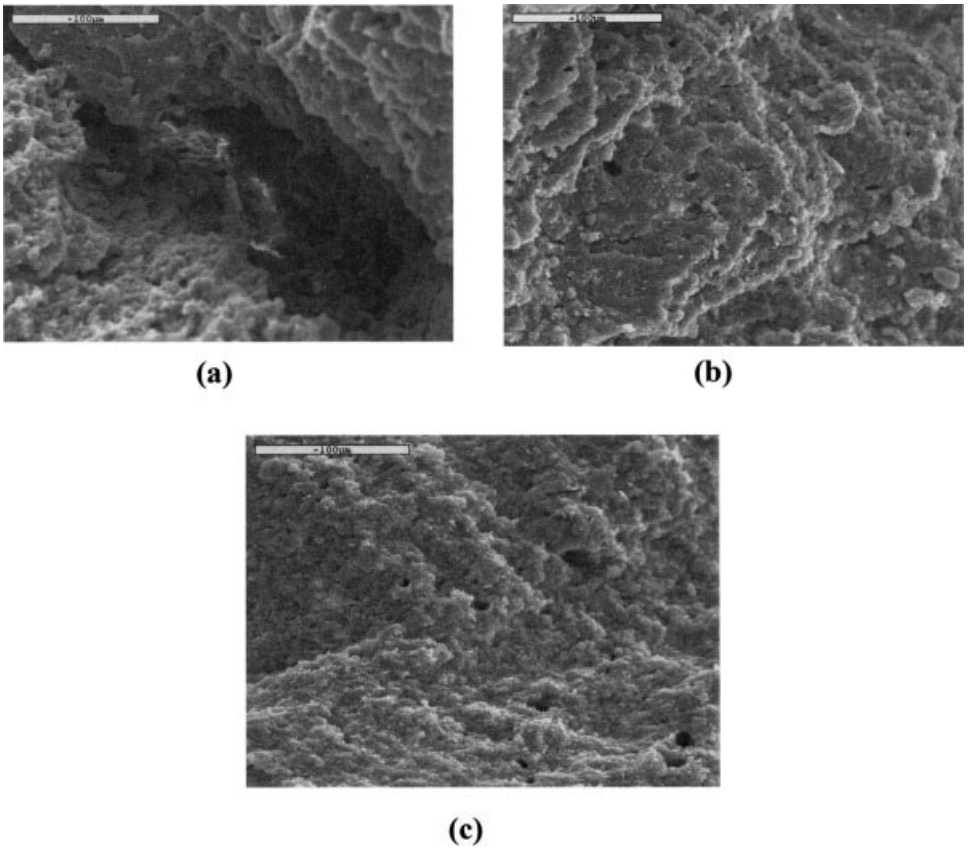

Figure 8 SEM fractography, ×400 of NR vulcanizates (a). Gum (b) with 5 phr organoclay and (c) with 10 phr organoclay.

size yielded rubber of higher molecular weight.[33] The nanocomposite containing 5 phr nanoclay exhibited higher tensile strength and elongation at break when compared with other compounds. A loading of 5–7 phr modified clay has been shown earlier[13] to impart high mechanical properties for NR nanocomosites. The magnitude of improvement in modulus increases with loading of clay up to 15 phr with the extensibility remaining little affected,[43] which proves that more rubber molecules are intercalated leading to better dispersion of clay with formation of a more homogeneous network. The hardness values are in agreement with other mechanical properties.

The observed improvements in mechanical properties of NR nanocomposites are supported by the SEM fractography of the samples as well. With the addition of OC, the otherwise smooth fracture with catastrophic failure mode of the gum sample [Fig. 8(a)] changes to highly deviated crack paths, which interact with each other leading to parabolic patterns [Figs. 8(b) and 8(c)].

The results of thermal aging (70°C, 6 days) of NR nanocomposites are given in Table VII. The aged modulii, tensile strength, and elongation at break

TABLE VII
Mechanical Properties of Aged Skim NR

Parameter	Loading of clay (phr)				
	0	1	3	5	10
Modulus,100% (MPa)	1.81	2.02	2.14	2.23	2.85
Modulus, 200% (MPa)	2.96	3.27	3.21	3.82	3.69
Modulus, 300% (MPa)	4.02	4.08	4.5	4.8	5.00
Tensile strength (MPa)	24.34	25.5	24.8	24	24.6
Elongation at break (%)	630	700	700	740	650

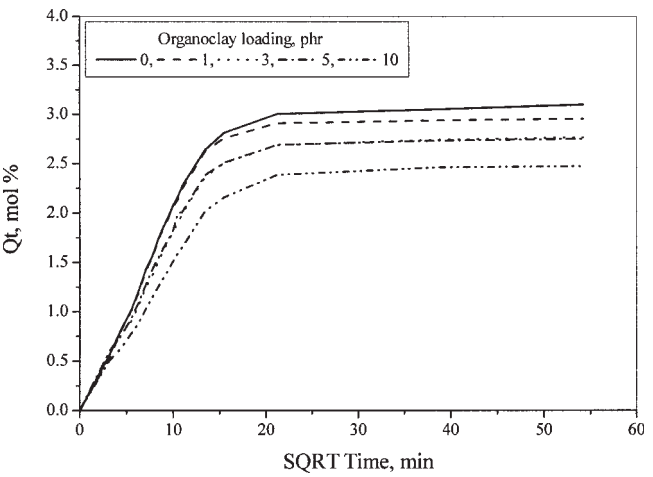

Figure 9 Swelling behavior of clay filled nanocomposites in toluene at 20°C.

TABLE VIII
TGA Data of NR Nanocomposites

Clay loading (phr)	Max. degradation temperature (°C)	Percent weight retained			
		200[a]	300	400	500
0	374.5	98.66	91.84	32.29	10.58
2	375.0	98.57	90.34	33.05	11.30
3	375.0	98.79	91.35	33.28	11.65
5	375.0	98.54	90.79	34.89	12.25
10	375.0	98.61	90.47	36.65	14.95

[a] 200, 300, 400, and 500 are the different temperatures (in °C).

show negligible changes when compared with unaged samples, thus proving the better thermal ageing properties of the nanocomposites.

Solvent swelling

The sorption curves of nanocomposites obtained by plotting Q_t (mole percent of toluene absorbed per 100 g of composite) in toluene at 20°C is shown in Figure 9.

Comparatively low swelling is observed for gum vulcanizate, suggesting a good level of crosslinking as obtained from the rheographs. The solvent absorbed decreases with increased loading of clay. The rate of solvent transport is reduced by the presence of impermeable clay layers.

Thermal behavior

The thermal characteristics of NR nanocomposites are given in Table VIII. The maximum degradation temperature is shown to be independent of the presence and concentration of OC. However, at 400°C the percentage retained is higher for the nanocomposites. Higher residue is also retained for all the nanocomposites and increases in proportion with clay. The enhanced thermal resistance is attributed to the good dispersion of OC in the rubber matrix as reported.[16]

CONCLUSIONS

A simple and environmentally friendly procedure was standardized for production of NR nanocomposites from skim latex produced as a by-product during centrifugation of NR latex. Creaming of skim NR latex resulted in a reduction of the rubber particle size and also in an easier coagulation by acids. The rubber recovered from acid coagulated, clay mixed latex had good color and could be processed like conventional rubber vulcanizate. XRD results revealed that there was an increase in the basal spacing between the clay layers because of intercalation of NR molecules, leading to better polymer filler interaction. NR chains, because of their very high segmental mobility, were able to intercalate into the gap very easily and cause exfoliation, as observed from TEM images. The presence of OC resulted in a faster onset of cure and higher level of crosslinking. A better dispersion of modified clay, together with the higher level of crosslinking, resulted in enhanced mechanical properties and ageing characteristics. As nanocomposites were prepared from latex directly, comparatively high strength values were observed for NR. Because of the higher level of polymer filler interaction, there was a deviation of fracture path of NR, as observed from SEM micrographs. This also resulted in increased resistance to swelling by solvents.

Rosamma Alex is grateful to KOSEF and KOFST for the Brain Pool Scientist award.

References

1. Southorn, R. A. In Proceedings of Natural Rubber Research Conference (1960); Rubber Research Institute of Malaya: Kuala Lumpur, 1961; p 766.
2. Gomez, J. B.; Moir, G. K. J. Monograph No. 4; Malaysian Rubber Research and Develpoment Board: Kuala Lumpur, 1979.
3. Du Pont, J.; Moreau, P.; Lance, C.; Jacob, J. L. Phytochem 1976, 15, 1219.
4. Hasma, H.; Subramanium, A. J Nat Rubber Res 1986, 1, 30.
5. Hasma, H. J Nat Rubber Res 1991, 6, 105.
6. Mathew, N. M.; Claramma, N. M. In Latex Preservation and Concentration in Natural Rubber: Agromanagement and Crop Processing; George, P. J.; Kuruvila, C., Eds.; Rubber Research Institute of India: Kottayam, 2000; p 426.
7. Kuriakose, B. In Natural rubber: Biology, Cultivation and Technology; Sethuraj, M. R.; Mathew, N. M., Eds.; Elsevier: Amsterdam, 1992; Chapter 17.
8. Chiew Sum, N. G. J Rubber Res Inst Malaysia 1983, 31, 49.
9. Ong, C. O. In Proceedings of the Rubber Research Institute of Malaysia, Planters Conference, Kuala Lumpur, Malaysia, 1974; p 243.
10. Sakdapipanich, J. T.; Nawamawati, K.; Tanaka, Y. J Rubber Res 2002, 5, 1.
11. Kojima, Y.; Usuki, A.; Kawasumi, M.; Okada, A.; Kurauchi, T.; Kamigaito, O. J Appl Polym Sci 1993, 49, 1259.
12. Giannelis, E. P. Adv Mater 1996, 8, 29.
13. Magaraphan, R.; Thaijaroen, W.; Lim-Ochakun, R.. Rubber Chem Technol 2003, 76, 406.
14. Mouri, H.; Akutagawa, K. Rubber Chem Technol 1999, 72, 960.
15. Vaia, R. A.; Vasudevan, S.; Krawiec, W.; Scanlon, L. G.; Giannelis, E. P. Adv Mater 1995, 7, 154.
16. Ganter, M.; Gronski, W.; Reichert, P.; Mulhaupt, R. Rubber Chem Technol 2001, 74, 221.
17. Lopez-Manchado, M. A.; Herrero, B.; Arroyo, M. Polym Int 2004, 53, 1766.
18. Sadhu, S.; Bhowmick, A. K. Adv Eng Mater 2004, 6, 738.
19. Wu, Y.-P.; Wang, Y.-Q.; Zahng, L.-Q. Macromol Mater Eng 2004, 289, 890.
20. Acharya, H.; Pramanik, M.; Srivastava, S. K.; Bhowmick, A. K. J Appl Polym Sci 2004, 93, 2429.
21. Teh, P. L.; Mohd Ishak, Z. A.; Hashim, A. S.; Karger-Kocsis, J.; Ishiaku, U. S. J Appl Polym Sci 2004, 94, 2438.

22. Gatos, K. G.; Thomann, R.; Karger-Kocsis, J. Polym Int 2004, 53, 1197.
23. Ping, J. M.; You, X.; Mai, W.; Zhang, L. Q. Macromol Rapid Commun 2004, 25, 1692.
24. Wu, Y. P.; Zhang, L. Q.; Wang, Y. Z.; Liang, Y.; Yu, D. S. J Appl Polym Sci 2001, 82, 2842.
25. Zhang, L. Q.; Wang, Y. Z.; Wang, Y. Q.; Sui, Y.; Yu, D. S. J Appl Polym Sci 2000, 78, 1873.
26. Wang, Y.; Zhang, L.; Tang, C. H.; Yu, D. S. J Appl Polym Sci 2000, 78, 1879.
27. Wang, Y.; Zhang. H.; Wu, Y.; Yang, J.; Zhang, L. J Appl Polym Sci 2005, 96, 324.
28. Shell, J.; Wang, T.; Tokita, N.; Cabot, B. C. Rubber World 2000, 3, 40.
29. Alex, R.; Nah, C.; Mathew, G. Kor. Pat. No. 10-2005-0032843 (2005).
30. Roe, R. J. In Methods of X-Ray and Neutron Scattering in Polymer Science; Oxford University Press: New York, 2000; Chapter 3.
31. Rippel, M. M.; Lee, L.-T.; Carlos Leite, A. P.; Fernando Galembeck. J Colloid Interface Sci 2003, 268, 330.
32. Ohya, N.; Tanaka, Y.; Wititsuwannakul; Koyama, T. J Rubber Res 2000, 3, 214.
33. Singh, A. P.; Wi, S. G.; Chung, G. C.; Kim, Y. S.; Kang, H. J Exp Bot 2003, 54, 985.
34. Gomez, J. B.; Hamzah, S. J Nat Rubber Res 1985, 4, 204.
35. Andrews, E. H.; Dickenson, P. B. In Proceedings of Natural Rubber Research Conference (1960); The Rubber Research Institute of Malaya: Kula Lumpur, 1961; p 756.
36. Abdul Kader, M.; Nah, C. Polymer 2004, 45, 2237.
37. Vu, Y. T.; Mark, J. E.; Pham, L. H.; Engelhardt, M. J Appl Polym Sci 2001, 82, 1391.
38. Sharif, J.; Wan Md Zin Wan Yunus; Hj. Mohd Dahlan, K. Z.; Hj Ahmad, M. Polym Test 2005, 24, 211.
39. Tyan, H.-L.; Liu, Y.-C.; Wei, K.-H. Chem Mater 1999, 11, 1942.
40. Varghese, S.; Karger-Kocsis, J.; Gatos, K. G. Polymer 2003, 44, 3977.
41. Yeang, H. Y.; Yip, E.; Hamzah, S. J Nat Rubber Res 1995, 10, 108.
42. Subramaniam, A. RRIM Technol Bull 1980, 4, 20.
43. Varghese, S.; Karger-Kocsis, J. Polymer 2003, 44, 4921.